

Supporting Information

A toolbox of biodegradable dendritic (poly glycerol sulfate)-SS-poly(ester) micelles for cancer treatment: stability, drug release, and tumor targeting

Daniel Braatz,^a Mathias Dimde,^a Guoxin Ma,^a Yinan Zhong,^b Michael Tully,^a Carsten Grötzingen,^{c,d} Yuanyuan Zhang,^b Alexandros Mavroskoufis,^a Michael Schirner,^a Zhiyuan Zhong,^e Matthias Ballauff,^{a*} Rainer Haag^{a*}

^a Institut für Chemie und Biochemie, Freie Universität Berlin, Takustr. 3, 14195 Berlin, Germany

^b Department of Pharmaceutical Engineering, China Pharmaceutical University, Nanjing, 211198, P.R. China

^c Department of Hepatology and Gastroenterology, Charité Universitätsmedizin Berlin, Augustenburger Platz 1, 13353 Berlin, Germany

^d German Cancer Consortium (DKTK), partner site Berlin, 13353 Berlin, Germany

^e Biomedical Polymers Laboratory, College of Chemistry, Chemical Engineering and Materials Science, and State Key Laboratory of Radiation Medicine and Protection, Soochow University, Suzhou 215123, P.R. China

*Corresponding Authors

Email: mballauff@zedat.fu-berlin.de; haag@zedat.fu-berlin.de

Table of Contents

Synthesis of the hydrophobic block copolymer: PCL-COOH/PLGA-COOH/ PLA-COOH.....	1
Synthesis of the hydrophilic block copolymer: dPG-SS-NH ₂	1
Synthetic scheme of PCL/PLGA/PLG-COOH, dPG-SS-NH ₂ , and dPGS-SS-PCL/PLGA/PLA	3
Analytical data of the hydrophobic block copolymers: PCL/PLA/PLGA-COOH.....	4
Analytical data of the hydrophilic block copolymer: dPG-SS-NH ₂	7
Analytical data of the amphiphilic copolymers: dPGS-SS-PCL/PLA/PLGA	10
Serum stability of dPGS _{7.8} -SS-PCL _{7.8} micelles determined by FPLC	17
CMC plots dPGS-SS-PCL/PLA/PLGA micelles in PBS at 37 °C by DLS.....	20
Size distributions of dPGS-SS-PCL/PLA/PLGA micelles: DLS plot	21
Degradation in the presence of 10 mM GSH in PBS at 37 °C	21
Drug-Loading: Sunitinib-loaded micelles purified with SEC column (photography).....	23
Cellular Uptake of free Sunitinib and loaded in dPGS _{7.8} -SS-PCL _{7.8} micelles on HeLa cells.....	24
Cell viability on A549 cell line dPGS _{7.8} -SS-PCL _{7.8}	24
Cell viability on Vero E6 cell line dPGS _{7.8} -SS-PCL _{7.8}	25
Cell viability on HBE cell line dPGS _{7.8} -SS-PCL _{7.8}	25
Cell viability on L929 cell line dPGS _{7.8} -SS-PCL _{7.8}	26
Cell viability on HUVEC cell line dPGS _{7.8} -SS-PCL _{7.8} (Anti-Angiogenesis Assay)	26
References.....	27

03.03.2021

35

36 **Synthesis of the hydrophobic block copolymer: PCL-COOH/PLGA-COOH/**
 37 **PLA-COOH**

38 For the hydrophobic precursors, all polymerizations were conducted using organocatalysts,
 39 either DBU or TBD, by ring-opening polymerization of caprolactone, lactide, and
 40 glycolide under strict avoidance of metal catalysts such as Sn(oct)₂. It has been pointed out
 41 that traces of metal-based catalysts lead to toxicity of polymer systems.^{1, 2} The polymers
 42 were synthesized to obtain molecular weights of 4 and 8 kDa. The PCL-COOH was
 43 synthesized via TBD-mediated^{3, 4} polymerizations of ϵ -caprolactone initiated by ethanol.
 44 An adapted procedure of Hedrick *et al.* was performed to synthesize PLA-COOH.⁵ The
 45 synthesis of PLGA-COOH was obtained by conducting the following modified method of
 46 Hoye *et al.* under the use of DBU and sequential monomer addition of glycolide to yield a
 47 random-like distribution of lactide and glycolide.⁶ The ratio of lactide to glycolide was
 48 fixed as L:G 75:25. The addition of succinic anhydride quenched the reactions and
 49 introduced the carboxylic acid functional group (**Scheme 1**). For purification, the polymers
 50 got precipitated from acetone into cold methanol three times and dried under vacuum. The
 51 obtained polymers were analyzed by ¹H NMR and GPC (THF) (**Table S 1**).

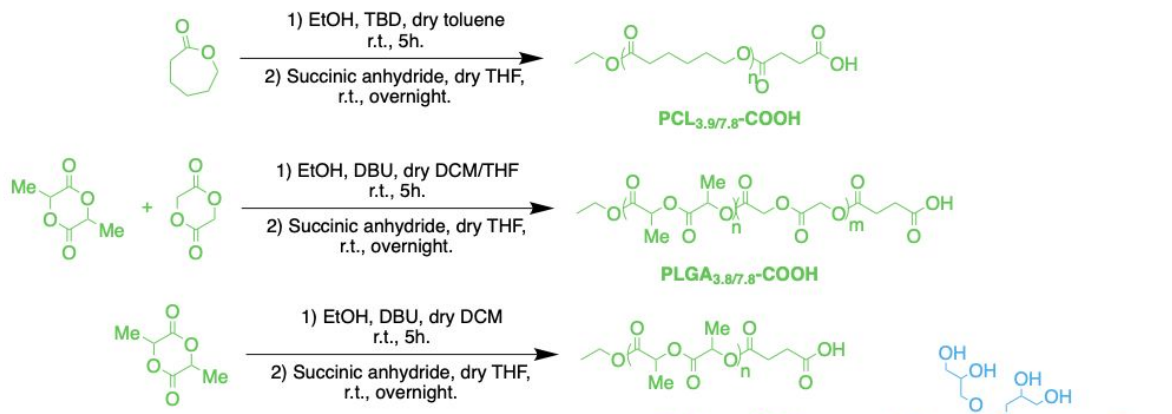
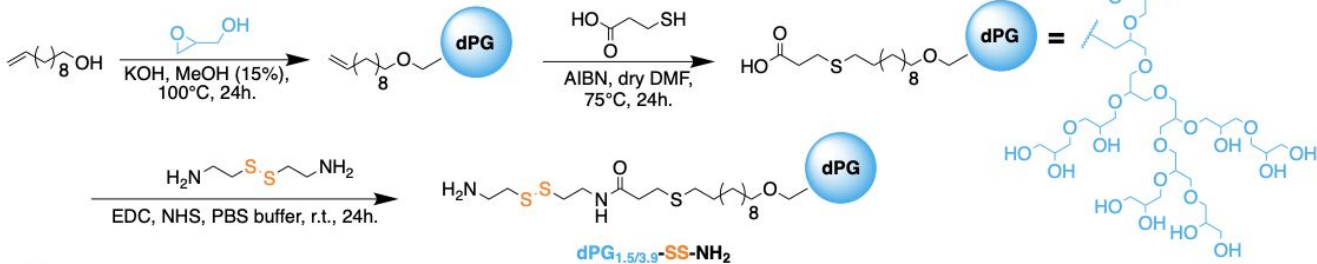
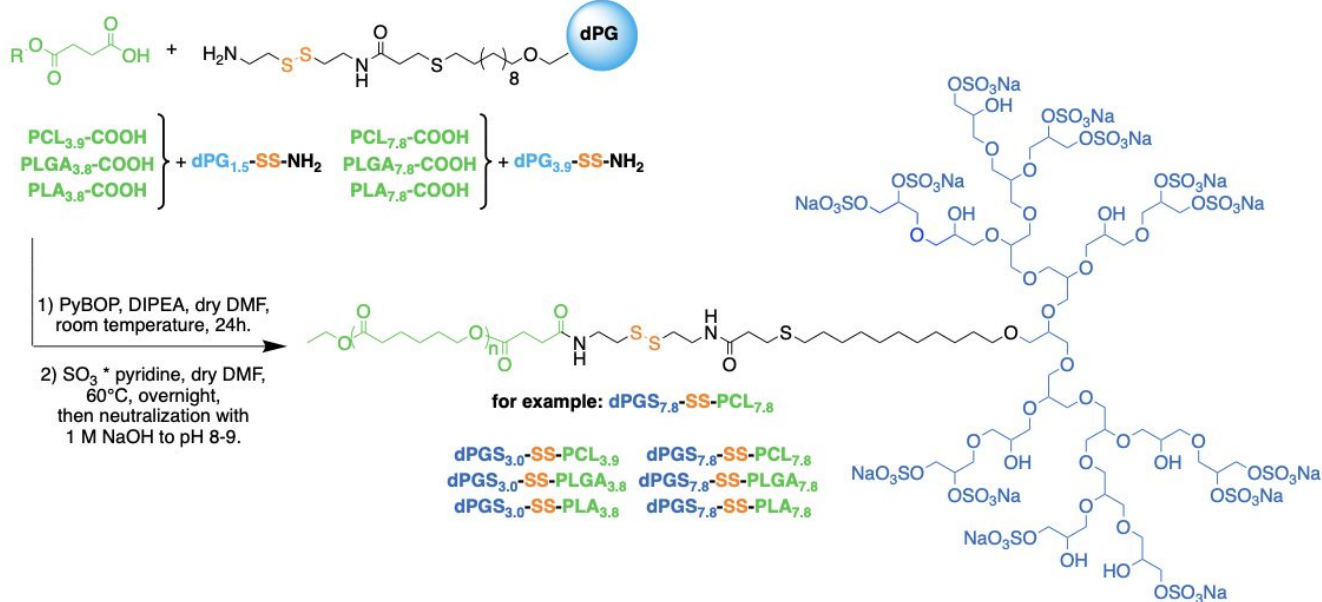
52

53

54 **Synthesis of the hydrophilic block copolymer: dPG-SS-NH₂**

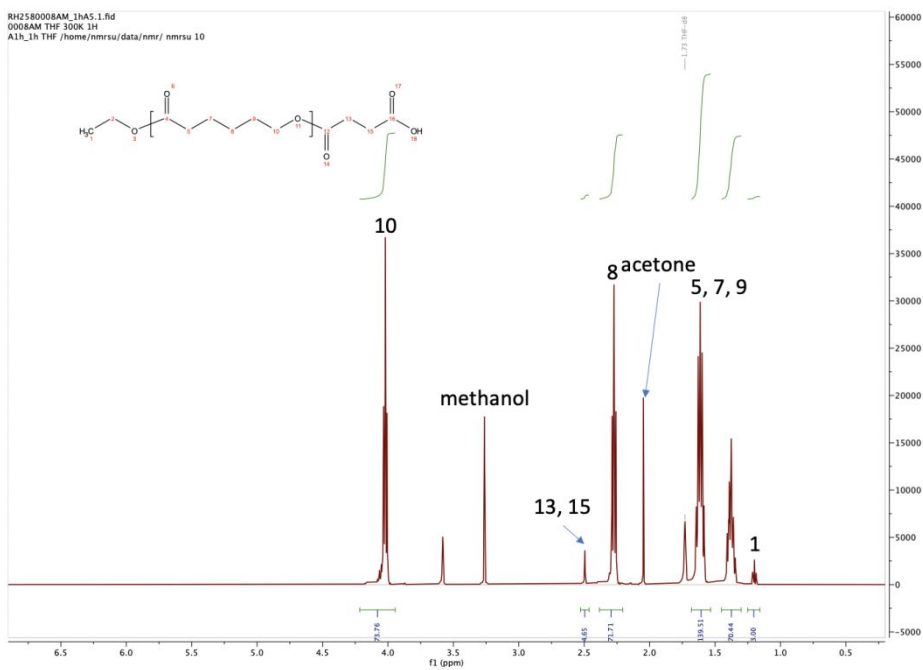
55 The hydrophilic polymers dPG-SS-NH₂ were targeted to yield molecular weights of either
 56 2 or 4 kDa. The hydrophilic segment presents as monofunctional dendritic polyglycerol,
 57 was synthesized through anionic ring-opening polymerization of glycidol initiated by
 58 10-undecenol-1-ol. The conversion of the reaction was monitored by ¹H NMR.
 59 Subsequently, the allyl group was modified by thiol-ene click-reaction of
 60 mercaptopropionic acid underuse of AIBN. The *in-situ* thiol-ene reaction to
 61 monofunctional dPG-thioether-COOH occurred within 4h. After purification by
 62 precipitation in acetone and TFF dialysis against water, the polymer was analyzed by GPC
 63 (water), revealing a molecular weight of 3.9 kDa and dispersity of 1.6 and 1.5 kDa and
 64 M_w/M_n of 1.6. The degree of branching in both cases reached almost 56%.⁷ Finally, to
 65 obtain amine end-capped copolymer capable of undergoing an amide coupling reaction,
 66 the dPG-thioether-COOH was reacted with Cystamine to either obtain amine end-capping
 67 as well as through implementation of
 68 Cystamine the redox-sensitive moiety present as disulfide bridge got introduced to the
 69 polymer structure. Therefore, monofunctional dPG-COOH was reacted with Cystamine
 70 underuse of EDC * HCl. After precipitation in acetone and running a TFF in water, the
 71 corresponding structure could be proven by ¹H NMR to obtain dPG-SS-NH₂ finally (**Table**
 72 **S 2**).

Synthetic scheme of PCL/PLGA/PLG-COOH, dPG-SS-NH₂, and dPGS-SS-PCL/PLGA/PLA

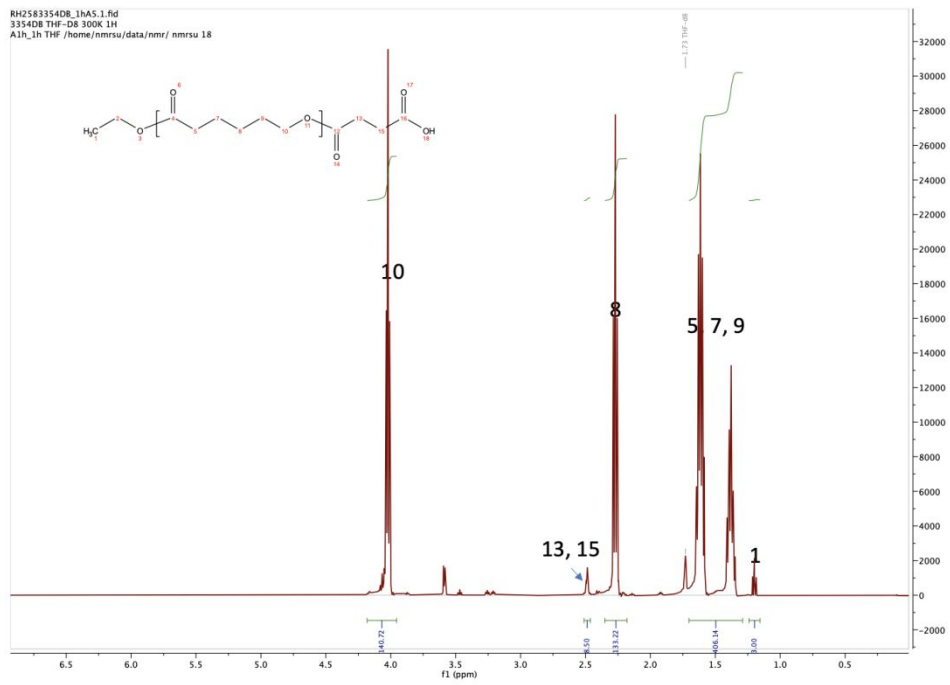
A**B****C**

76 **Scheme S 1.** synthetic pathways to **A)** hydrophobic segments of PCL/PLGA/PLA-COOH,
 77 **B)** hydrophilic segment of dPG-SS-NH₂, and **C)** amphiphilic block copolymers of
 78 dPGS-SS-PCL/PLGA/PLA.

Analytical data of the hydrophobic block copolymers: PCL/PLA/PLGA-COOH

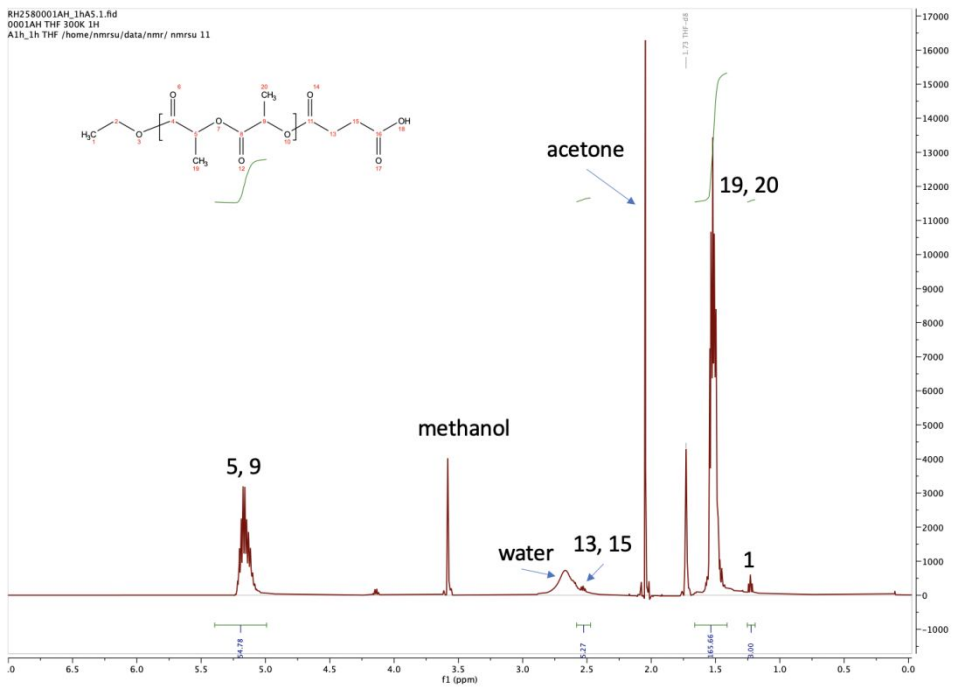


81 **Figure S 1.** ¹H NMR spectrum (500 MHz, THF-*d*₈) of PCL_{3.9}-COOH synthesized by ROP
82 of caprolactone with ethanol catalyzed by TBD.



84 **Figure S 2.** ¹H NMR spectrum (500 MHz, THF-*d*₈) of PCL_{7.8}-COOH synthesized by ROP
85 of caprolactone with ethanol catalyzed by TBD.

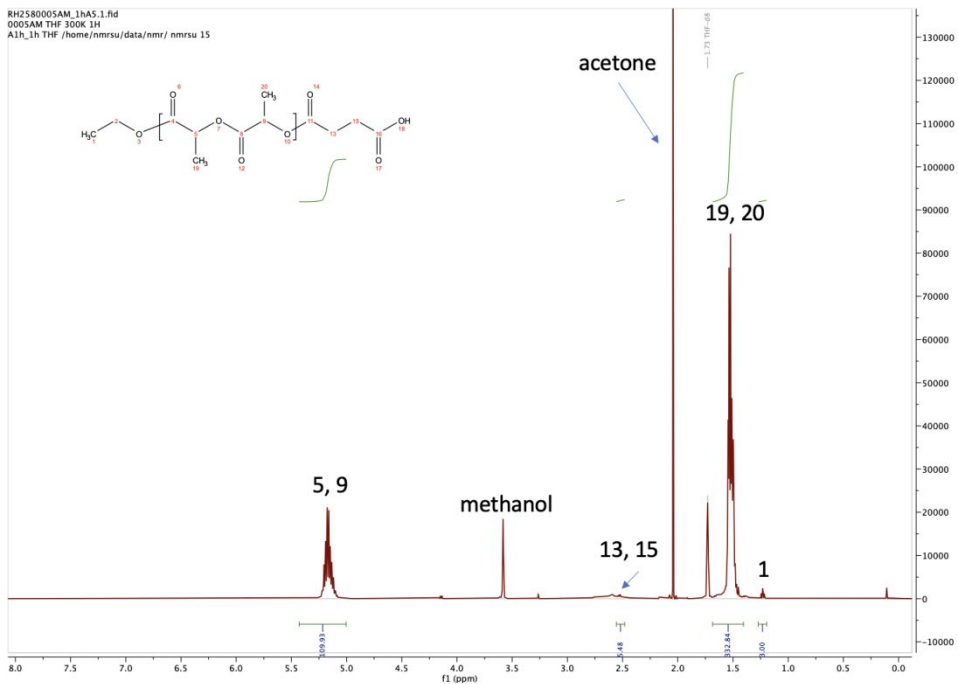
RH2580001AH_1hA5_1.fid
0001AH THF 300K 1H
A1h_1h THF /home/nmrstu/data/nmr/ nmrstu 11



86

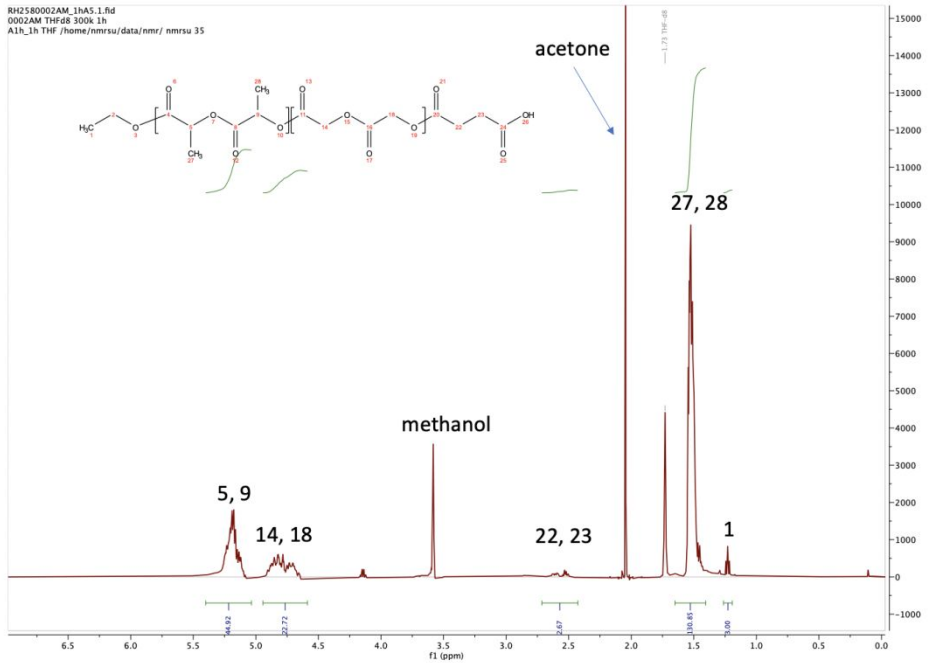
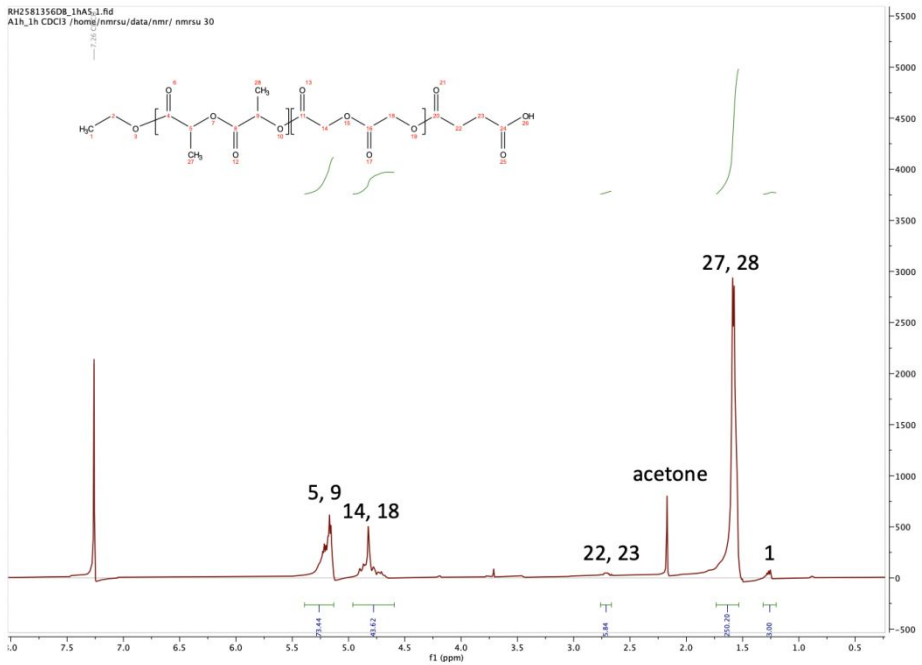
87 **Figure S 3.** ¹H NMR spectrum (500 MHz, THF-*d*₈) of PLA_{3.8}-COOH synthesized by ROP
88 of lactide with ethanol catalyzed by DBU.

RH2580005AM_1hA5_1.fid
0005AM THF 300K 1H
A1h_1h THF /home/nmrstu/data/nmr/ nmrstu 15



89

90 **Figure S 4.** ¹H NMR spectrum (500 MHz, THF-*d*₈) of PLA_{7.8}-COOH synthesized by ROP
91 of lactide with ethanol catalyzed by DBU.

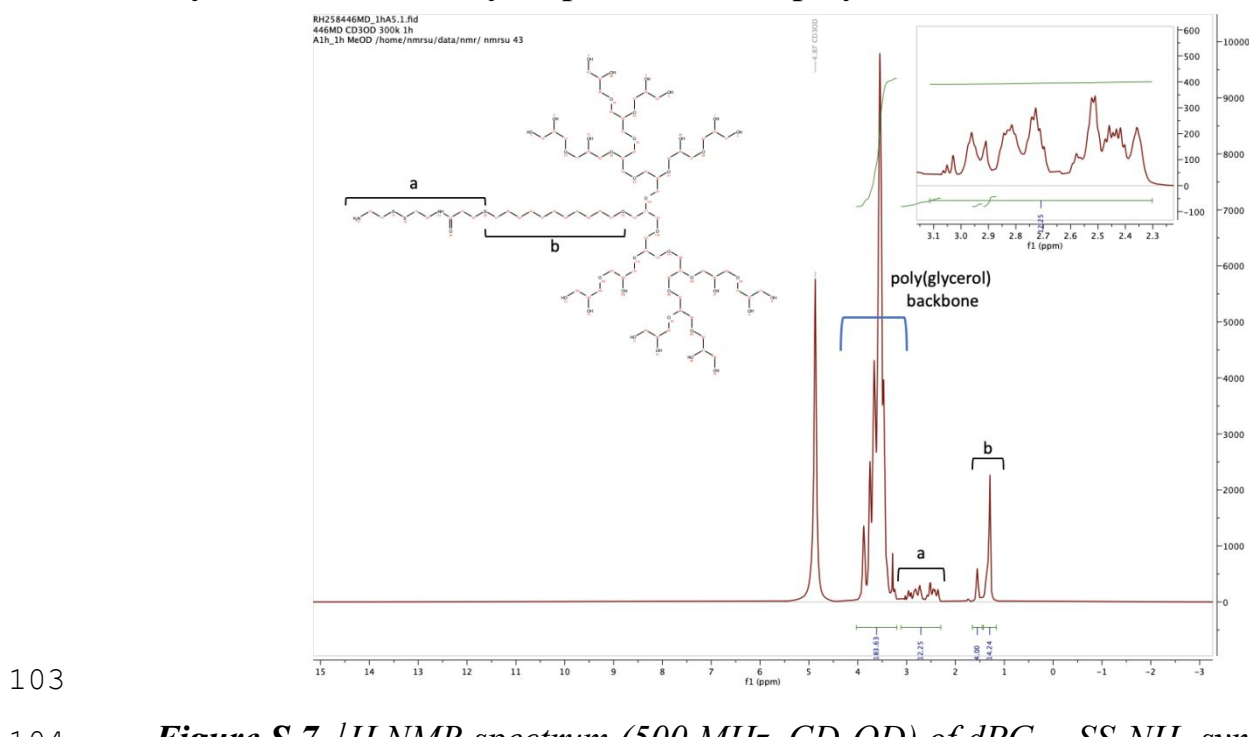


100
101

Table S 1. characteristics of PCL-COOH, PLA-COOH, and PLGA-COOH copolymers (^1H NMR, GPC).

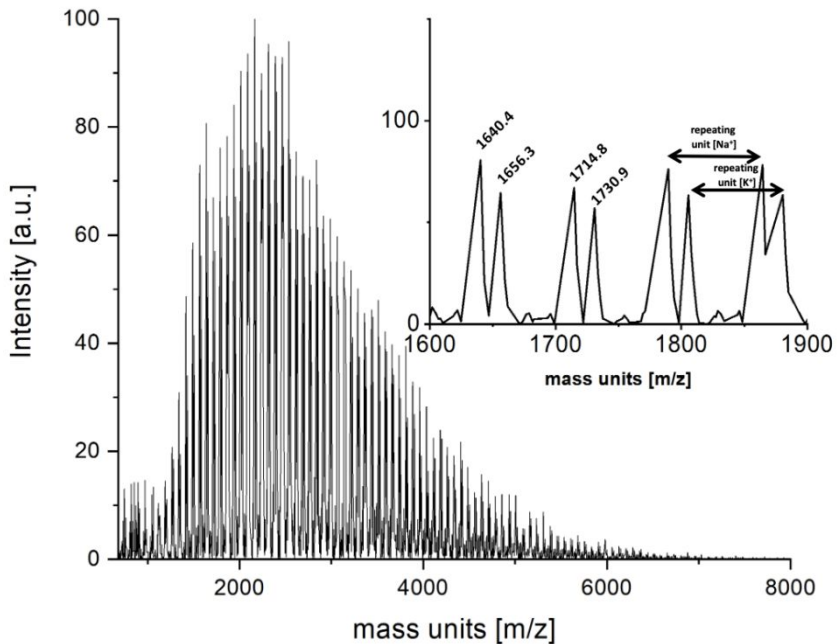
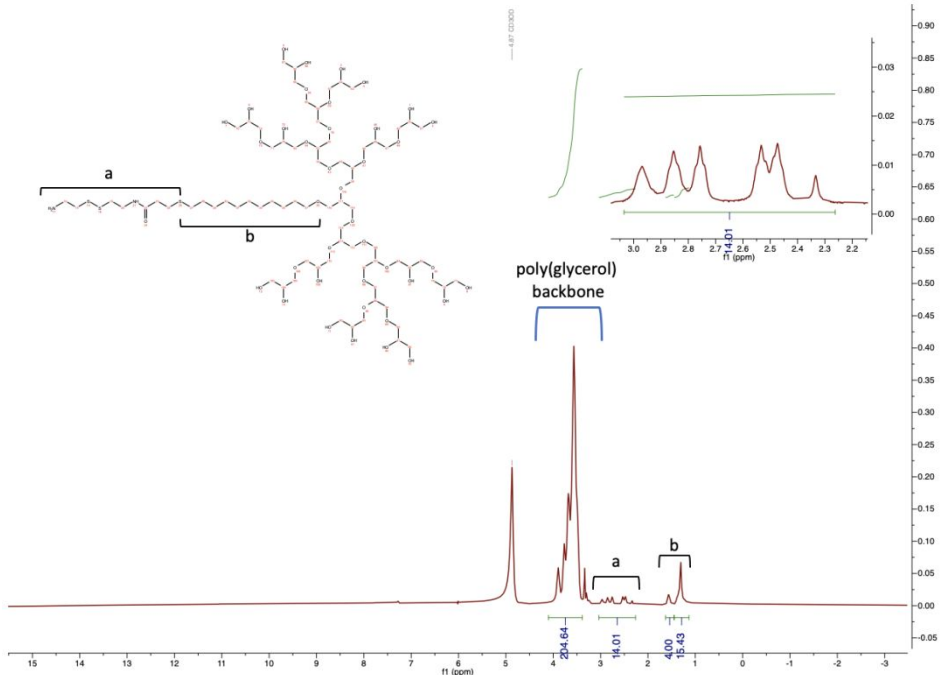
Compound	M_n (kDa)	theoretical	^1H NMR	GPC (THF)	D	Conversion (%)
PCL-COOH	8.0		7.8	9.8	1.15	98.8
PCL-COOH	4.0		3.9	7.1	1.42	99.7
PLA-COOH	8.0		7.8	12.1	1.29	98.6
PLA-COOH	4.0		3.8	9	1.38	97.5
PLGA-COOH	8.0		7.8	9.6	1.43	98.6
PLGA-COOH	4.0		3.8	7.7	1.36	97.5

102 **Analytical data of the hydrophilic block copolymer: dPG-SS-NH₂**



103

104 **Figure S 7.** ^1H NMR spectrum (500 MHz, CD₃OD) of dPG_{1.5}-SS-NH₂ synthesized by
105 ROP of glycidol from 10-undecenol with subsequent click-reaction of mercaptopropionic
106 acid and coupling of cystamine.



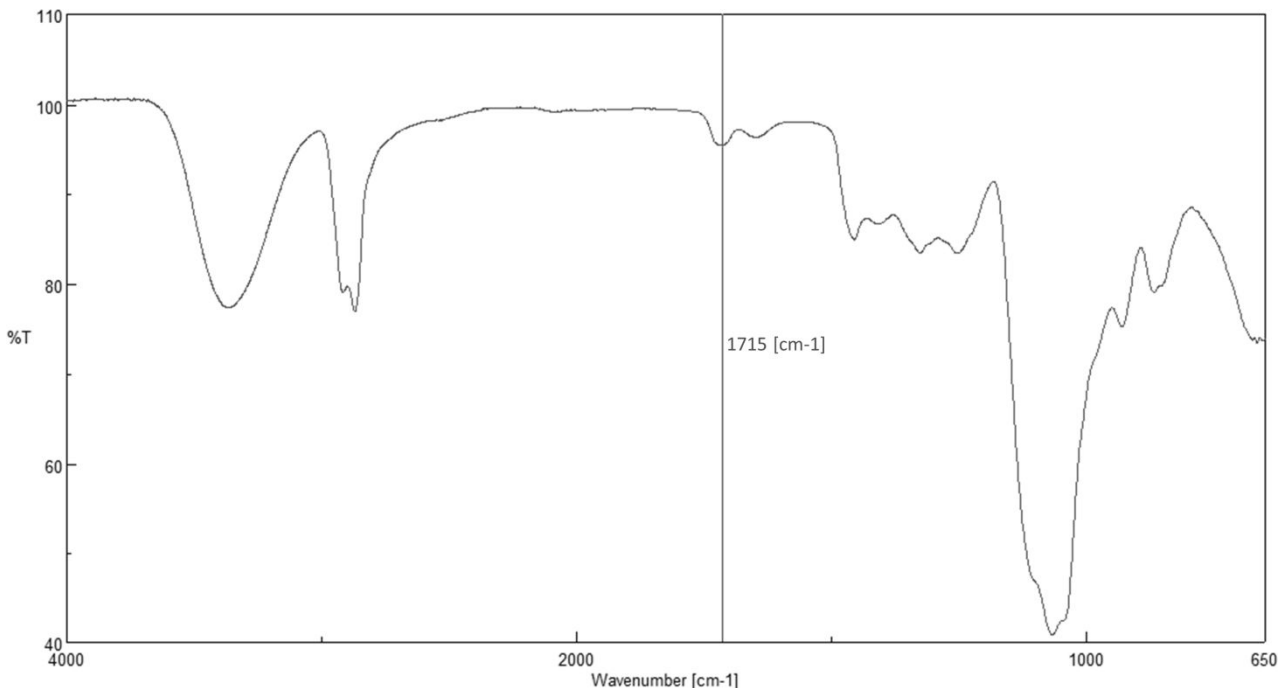


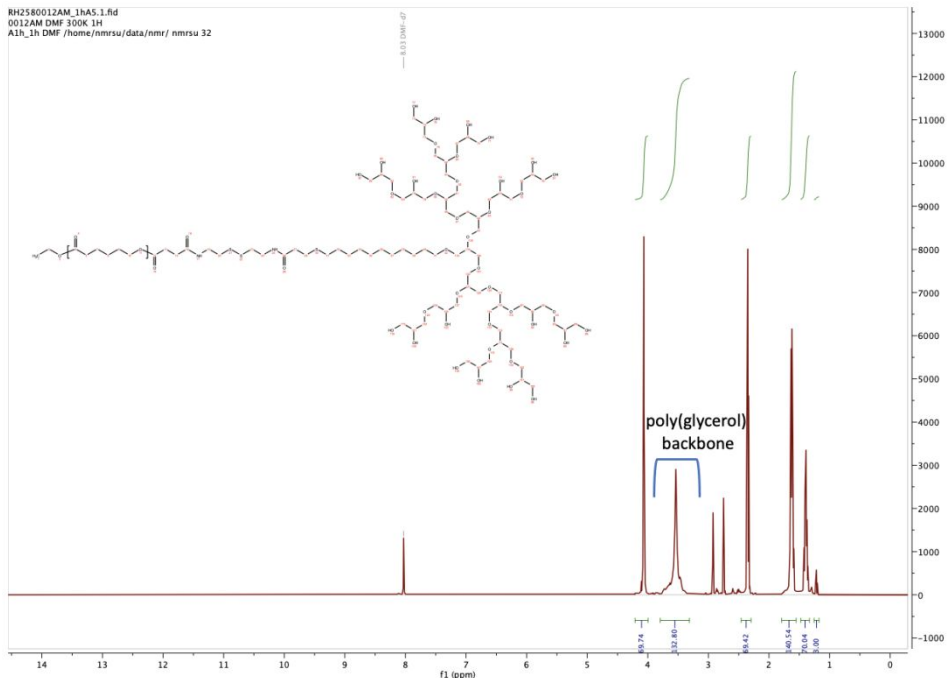
Figure S 10. IR spectrum of $dPG_{3.9}$ -COOH showing the characteristic ν_{as} ($C=O$) band at 1715 cm^{-1} .

Table S 2. characteristics of dPG -SS- NH_2 copolymers (1H NMR, Degree of branching by inverse gated ^{13}C NMR, GPC).

Compound	M_n (kDa)					Degree of Branching (%) ⁸
	theoretical	1H NMR	GPC (H_2O)	D		
dPG-SS-NH₂	4.0	3.4	3.9	1.63		58
dPG-SS-NH₂	2.0	1.6	1.5	1.59		56

123

Analytical data of the amphiphilic copolymers: dPGS-SS-PCL/PLA/PLGA

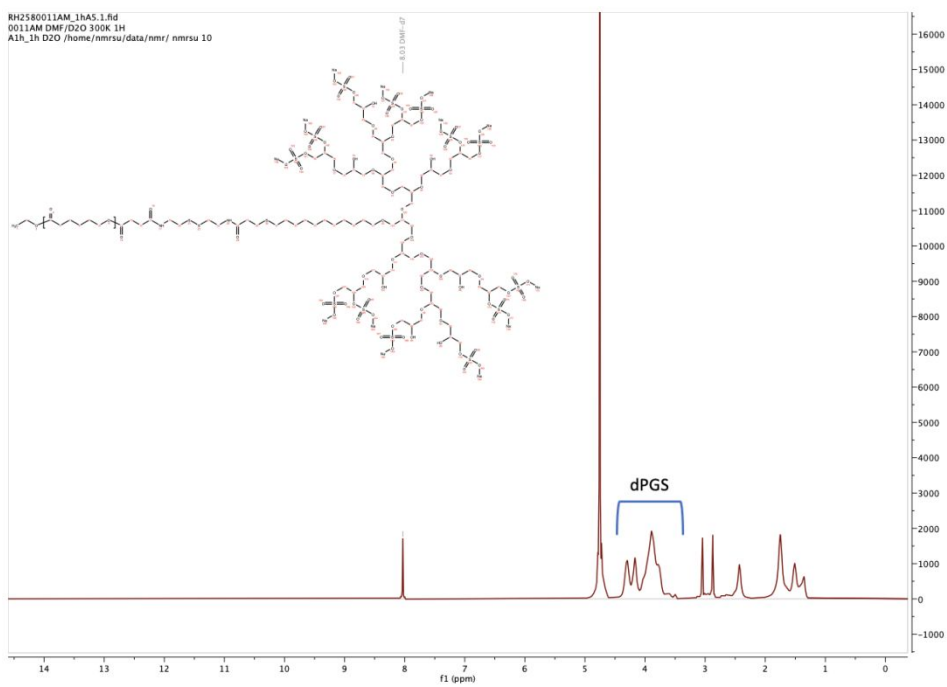


124

125

126

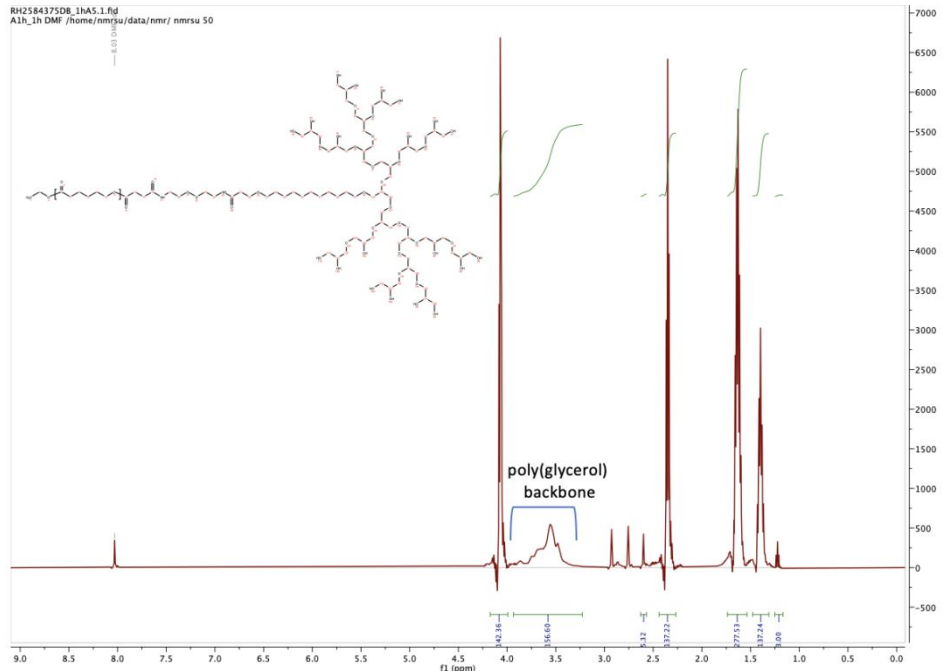
Figure S 11. ^1H NMR (500 MHz, DMF- d_7) of dPG_{1.5}-SS-PCL_{3.9} synthesized by amide coupling between dPG_{1.5}-SS-NH₂ and PCL_{3.9}-COOH.



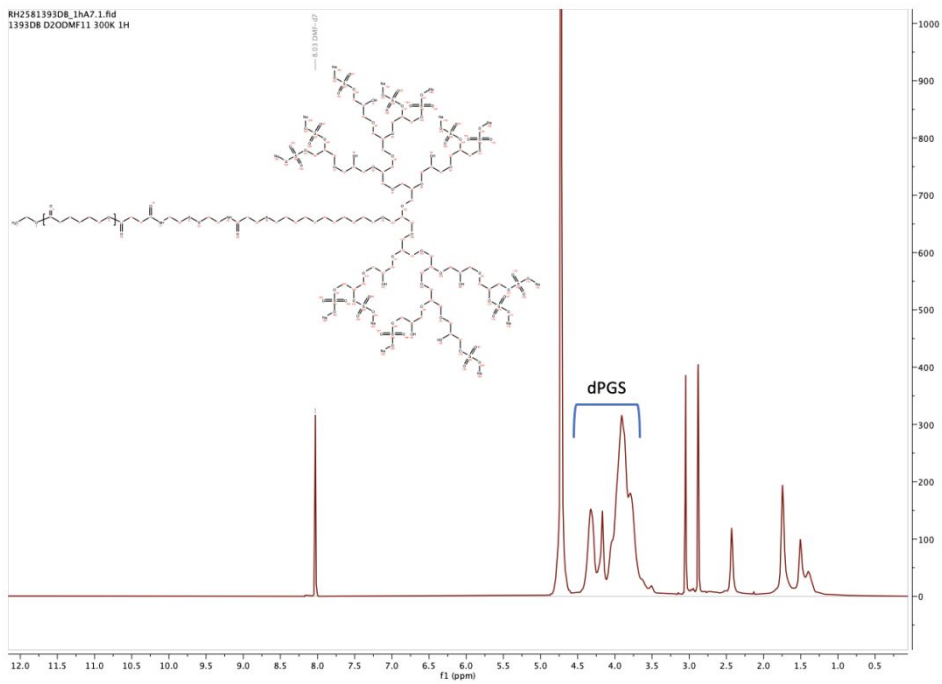
127

128

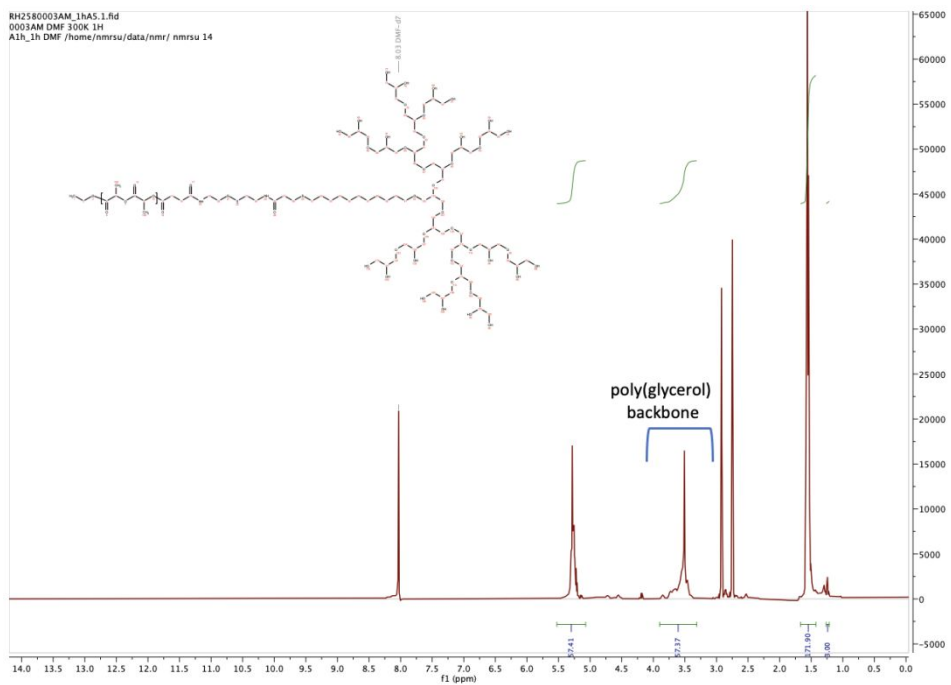
Figure S 12. ^1H NMR (500 MHz, DMF- d_7 :D₂O 1:1) of dPGS_{3.0}-SS-PCL_{3.9}.



130 **Figure S 13.** ^1H NMR (500 MHz, DMF- d_7) of $\text{dPG}_{3.9}\text{-SS-PCL}_{7.8}$ synthesized by amide
131 coupling between $\text{dPG}_{3.9}\text{-SS-NH}_2$ and $\text{PCL}_{7.8}\text{-COOH}$.

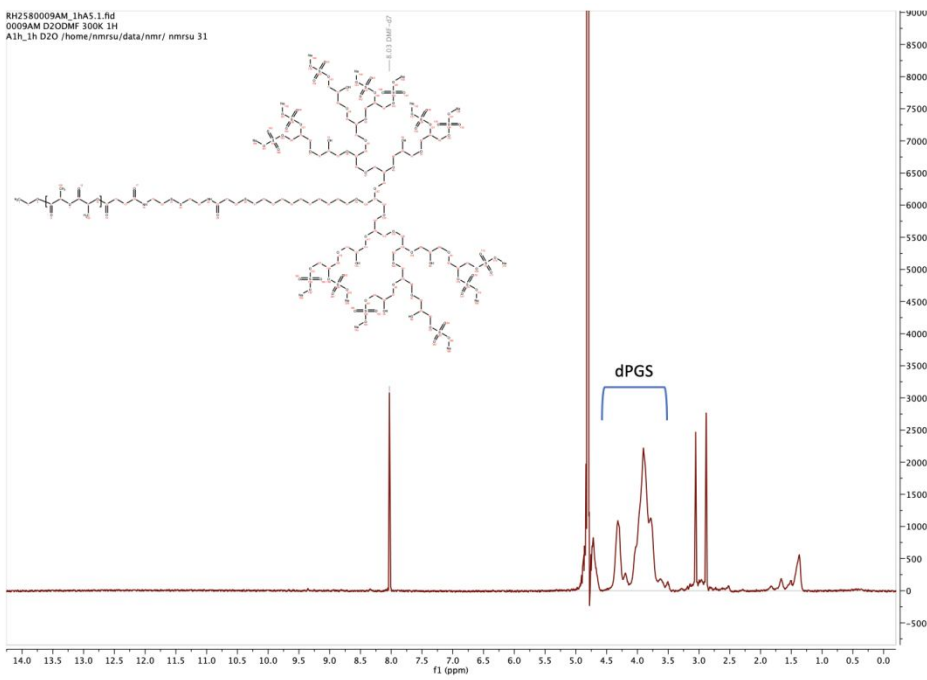


133 **Figure S 14.** ^1H NMR (500 MHz, DMF- d_7 : D_2O 1:1) of $\text{dPGS}_{7.8}\text{-SS-PCL}_{7.8}$.



134

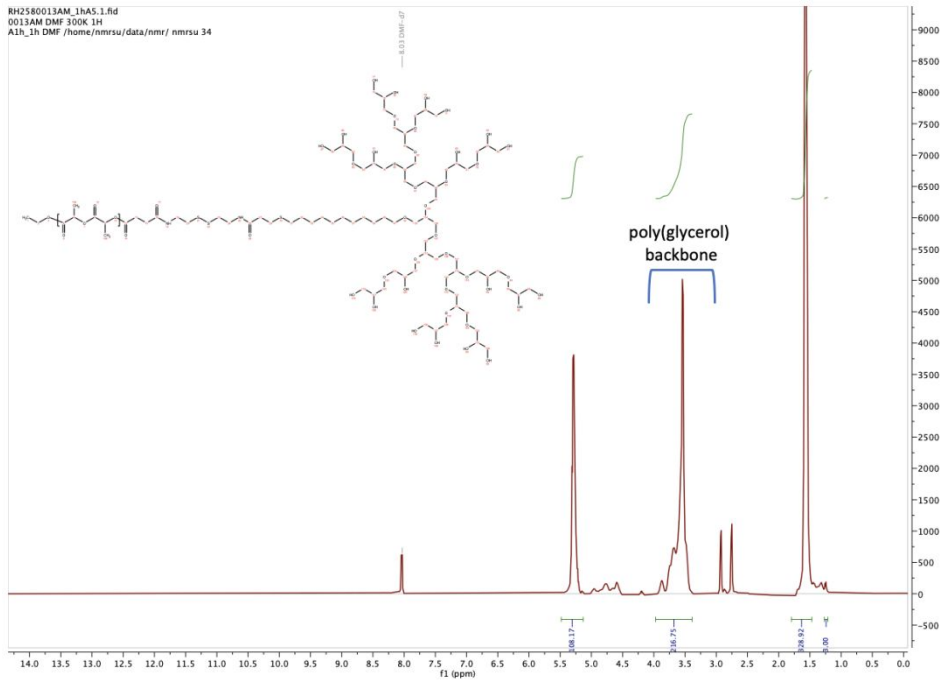
135 **Figure S 15.** ^1H NMR (500 MHz, DMF- d_7) of $d\text{PG}_{1.5}\text{-SS-PLA}_{3.8}$ synthesized by amide
136 coupling between $d\text{PG}_{1.5}\text{-SS-NH}_2$ and $\text{PLA}_{3.8}\text{-COOH}$.



137

138 **Figure S 16.** ^1H NMR (500 MHz, DMF- d_7 : $D_2\text{O}$ 1:1) of $d\text{PGS}_{3.0}\text{-SS-PLA}_{3.8}$.

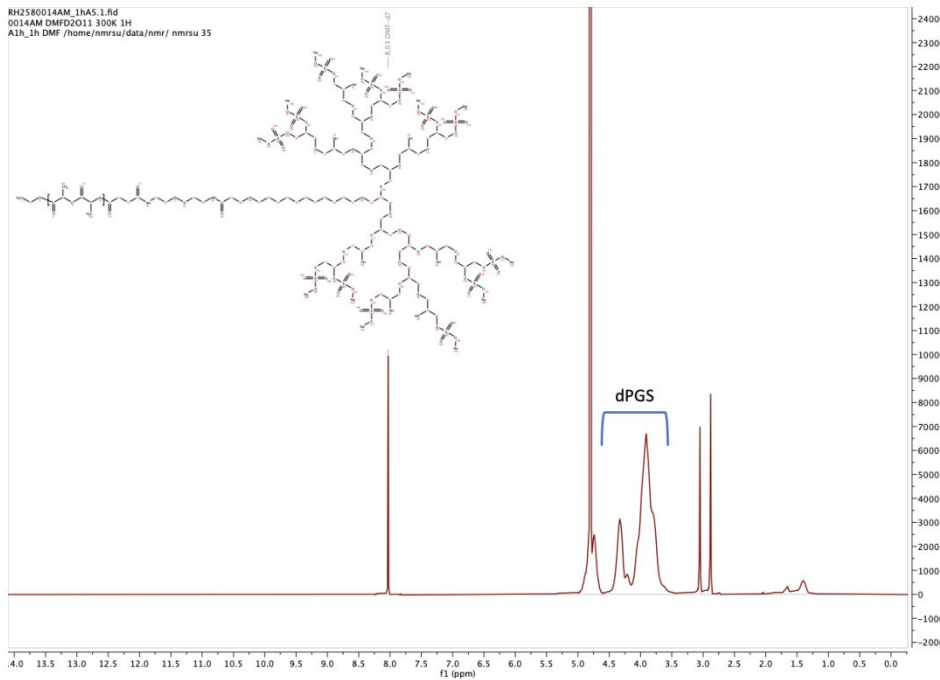
RH2580013AM_1hA5.1.fid
0013AM DMF 300K 1H
A1h_1h DMF /home/nmrssu/data/nmr/ nmrssu 34



139

140 **Figure S 17.** ¹H NMR (500 MHz, DMF-*d*₇) of dPG_{3.9}-SS-PLA_{7.8} synthesized by amide
141 coupling between dPG_{3.9}-SS-NH₂ and PLA_{7.8}-COOH.

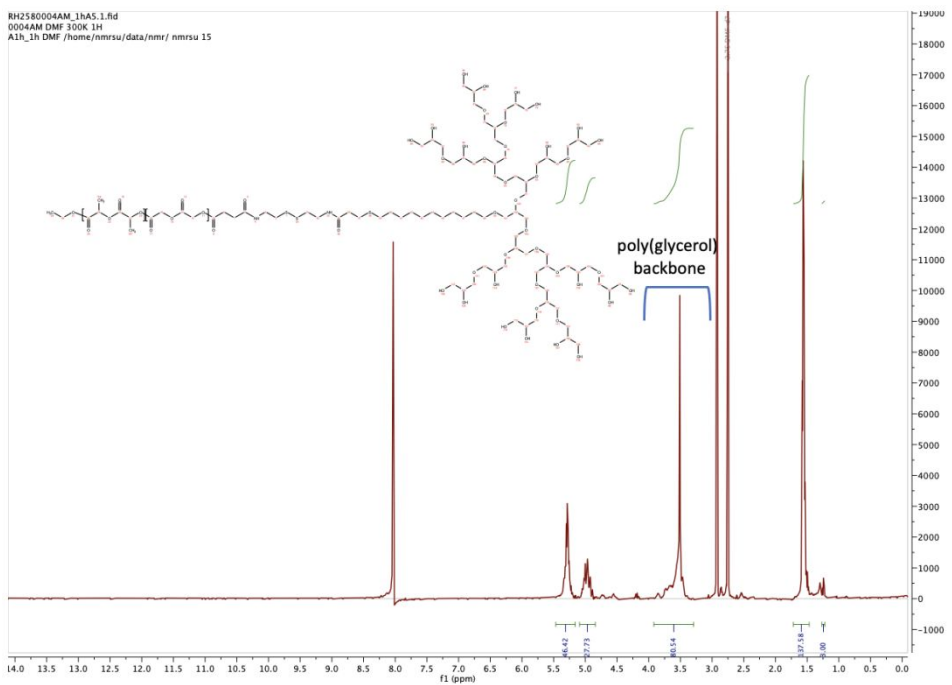
RH2580014AM_1hA5.1.fid
0014AM DMFD2011 300K 1H
A1h_1h DMF /home/nmrssu/data/nmr/ nmrssu 35



142

143 **Figure S 18.** ¹H NMR (500 MHz, DMF-*d*₇:D₂O 1:1) of dPGS_{7.8}-SS-PLA_{7.8}.

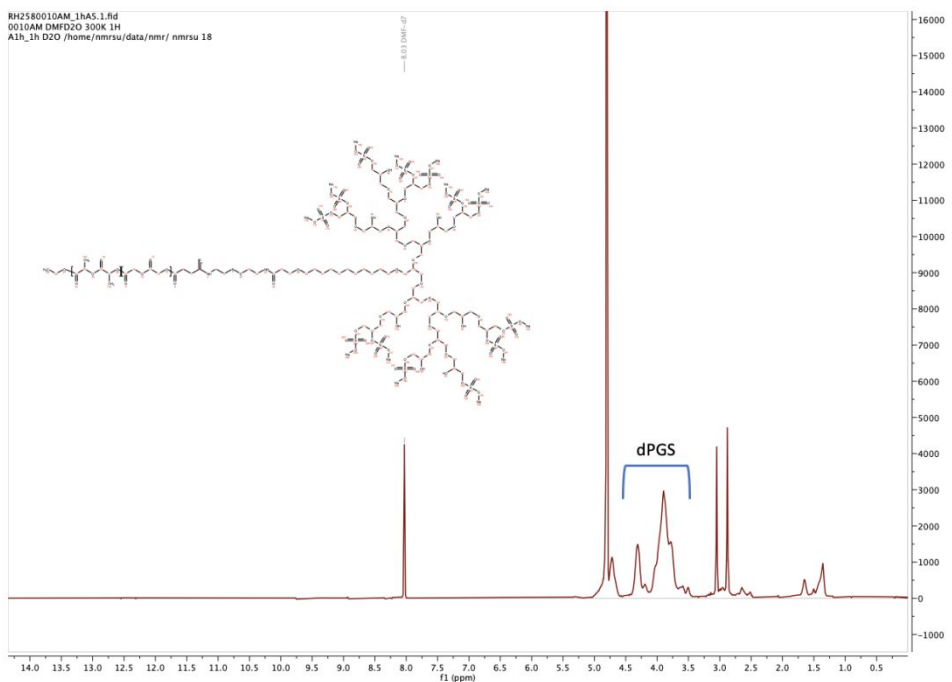
RH2580004AM_1hA5.1.fid
0004AM DMF 300K 1H
A1h_1h DMF /home/nmrsu/data/nmr/ nmrsu 15



144

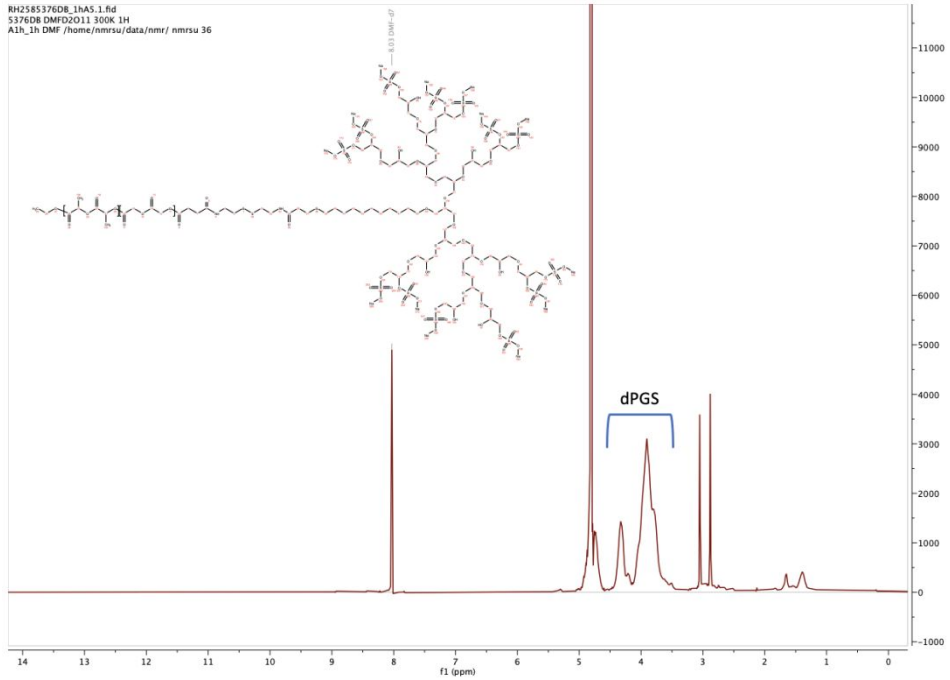
145 **Figure S 19.** ¹H NMR (500 MHz, DMF-*d*₇) of dPG_{1.5}-SS-PLGA_{3.8} synthesized by amide
146 coupling between dPG_{1.5}-SS-NH₂ and PLGA_{3.8}-COOH.

RH2580010AM_1hA5.1.fid
0010AM DMFD2O 300K 1H
A1h_1h D₂O /home/nmrsu/data/nmr/ nmrsu 18



147

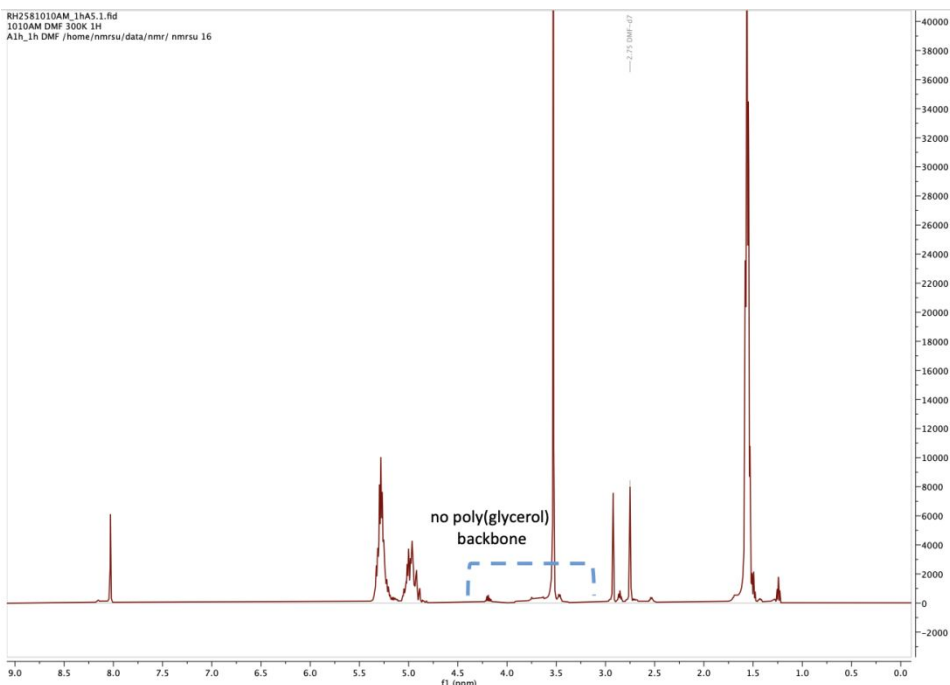
148 **Figure S 20.** ¹H NMR (500 MHz, DMF-*d*₇:D₂O 1:1) of dPGS_{3.0}-SS-PLGA_{3.8}.



149

150

Figure S 21. ^1H NMR (500 MHz, DMF- d_7 : $D_2\text{O}$ 1:1) of dPGS_{7.8}-SS-PLGA_{7.8}.



151

152

153

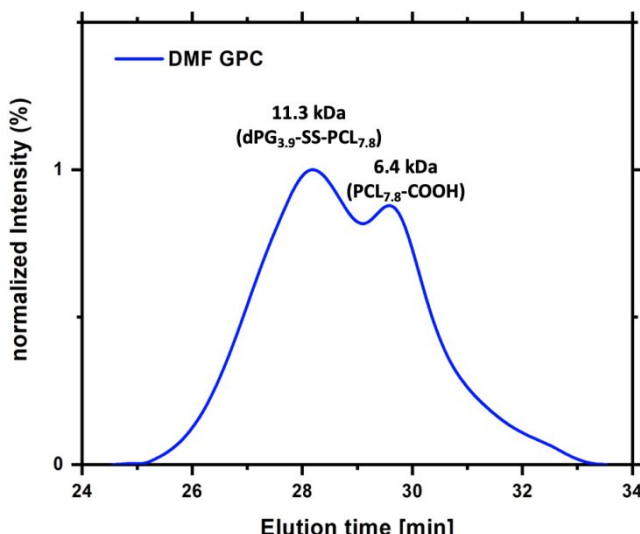
154

Figure S 22. precipitation of PLGA_{7.8}-COOH after sulfation of dPGS_{7.8}-SS-PLGA_{7.8} showing that separation was successful (no peaks of poly(glycerol); no dPGS_{7.8}-SS-PLGA_{7.8} in precipitation).

155
156**Table S 3.** characteristics of dPG-SS-PCL/PLA/PLGA. (*sulfation was run directly conducted after coupling)

Compound	M_n (kDa)			
	theoretical	^1H NMR	GPC (DMF)	D
dPG _{3.9} -SS-PCL _{7.9}	12	10.3	11.3	1.62
dPG _{1.5} -SS-PCL _{4.0}	6	5.9	11.7	1.43
dPG _{3.9} -SS-PLA _{7.9}	12	10.1	13.8	2.05
dPG _{1.5} -SS-PLA _{3.9}	6	4.9	13.6	1.48
dPG _{3.9} -SS-PLGA _{7.9}	12	-*	-*	-*
dPG _{1.5} -SS-PLGA _{3.9}	6	5.3	10.7	1.48

157



158

159
160
161**Figure S 23.** GPC chromatogram of dPG_{3.9}-SS-PCL_{7.8} after amide coupling (main peak: dPG_{3.9}-SS-PCL_{7.8}, shoulder: non-coupled PCL_{7.8}-COOH; depicted molecular weights are according to the GPC results).162
163**Table S 4.** degree of sulfation of dPGS-SS-PCL/PLGA/PLA copolymers according to elemental analysis.

Compound	theoretical		Degree of sulfation (%)
	S content (%)	^{100%} functionalization	
dPGS _{7.8} -SS-PCL _{7.8}	14.7	11.4	78%
dPGS _{3.0} -SS-PCL _{3.9}	12.9	10.4	81%
dPGS _{7.8} -SS-PLA _{7.8}	14.7	11.6	79%
dPGS _{3.0} -SS-PLA _{3.8}	12.6	12.3	97%
dPGS _{7.8} -SS-PLGA _{7.8}	14.2	12.6	89%
dPGS _{3.0} -SS-PLGA _{3.8}	15.0	13.0	87%

Serum stability of dPGS_{7,8}-SS-PCL_{7,8} micelles determined by FPLC

Table S 5. serum stability of dPGS_{7.8}-SS-PCL_{7.8} micelles detected by FPLC; micelles were incubated with 45 mg/mL HSA in PBS at 37 °C for 0 h or 24 h and loaded on a Superdex 200 10/30 column; the calculated peak areas were normalized to 0 h giving the serum stability in percentages.

Peak integral					n = 3			
Time (h)	micelle	HSA 1	HSA 2	HSA 3	Micelle/HSA	Micelle/HSA Average	normalized to 0h	micellar stability (%)
0	46.16	104.15	349.53	104.42	0.083			
0	46.27	101.14	360.23	84.60	0.085	0.083	1.000	
0	41.68	88.00	350.04	74.31	0.081			
24	40.85	89.69	329.60	100.72	0.079			
24	39.62	89.67	321.21	128.50	0.073	0.078	0.940	94.0
24	43.81	85.89	361.40	87.49	0.082			

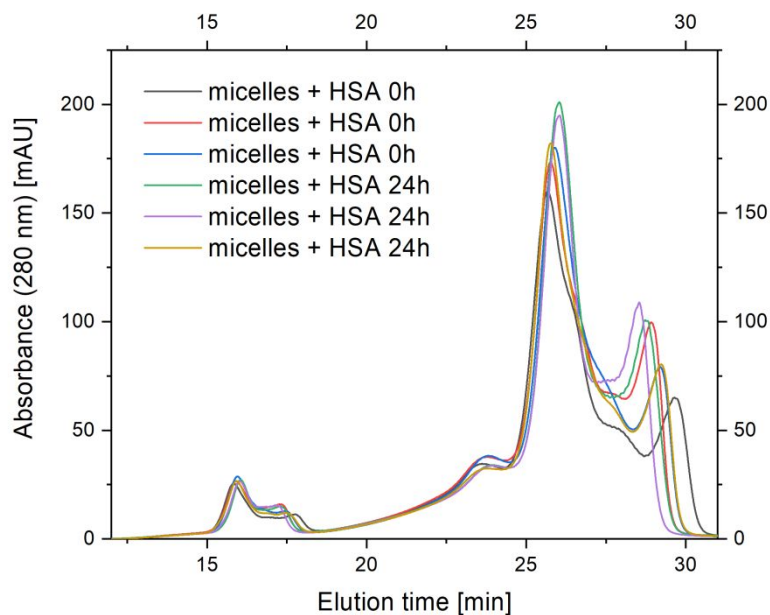
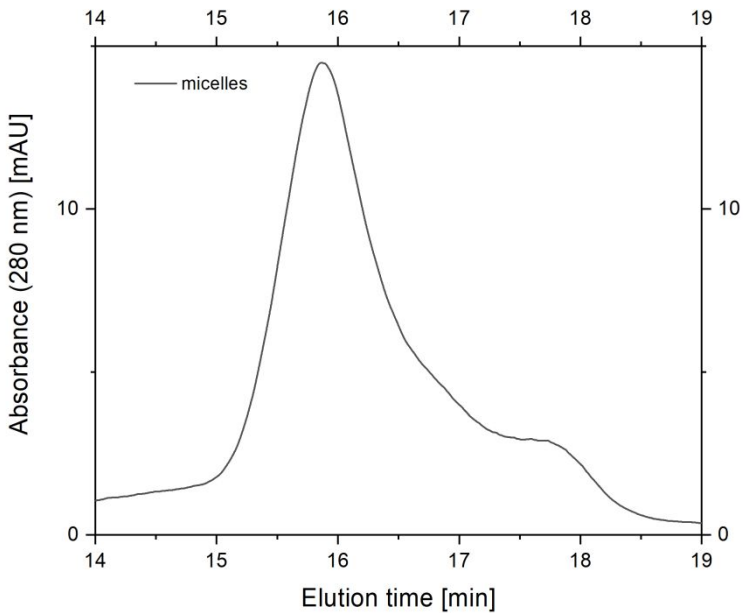


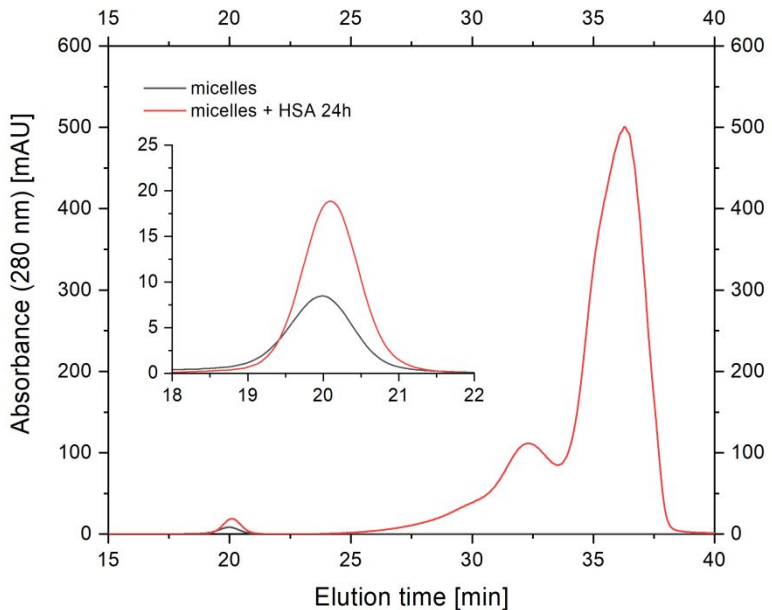
Figure S 24. FPLC chromatograms at 280 nm of dPGS_{7.8}-SS-PCL_{7.8} micelles (8 mg/mL) incubated with 45 mg/mL HSA in PBS at 37 °C (micelles: 15–18 min; HSA: 18–30 min) ($n = 3$).



173

174
175

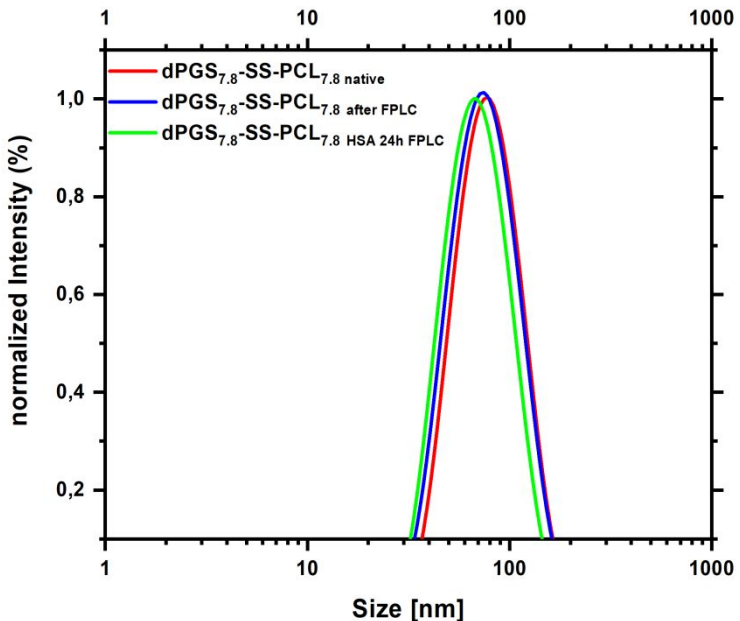
Figure S 25. SEC traces at 280 nm of dPGS_{7.8}-SS-PCL_{7.8} micelles (Elution time: 15 – 18 min; concentration 8 mg/mL).



176

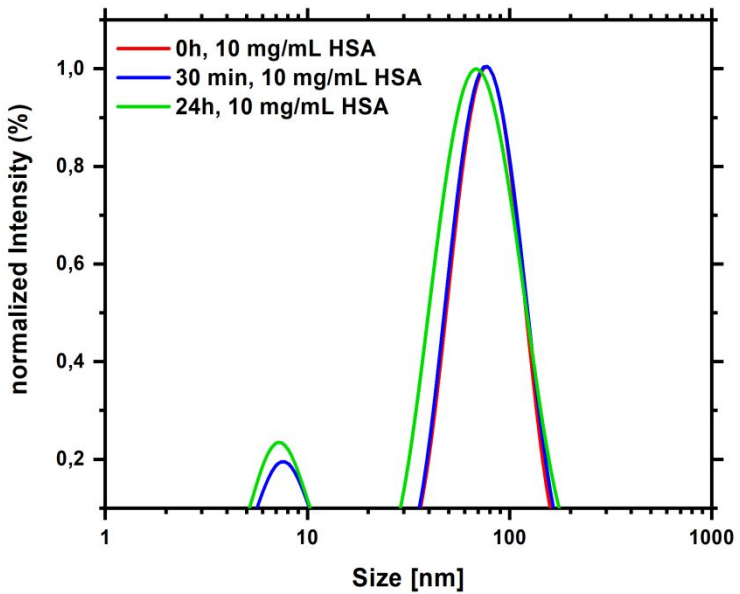
177
178

Figure S 26. SEC traces at 280 nm of dPGS_{7.8}-SS-PCL_{7.8} (1 mg/mL) alone and incubated with HSA (10 mg/mL) for 24 h.



179

180 **Figure S 27.** the size distribution of dPGS_{7.8}-SS-PCL_{7.8} micelles before and after SEC
181 separation from HSA shows that micelle size is not affected either by SEC or
182 protein incubation.



183

184 **Figure S 28.** the size distribution of dPGS_{7.8}-SS-PCL_{7.8} micelles incubated with 10 mg/mL
185 HSA in PBS at 37 °C showing no size change of micelles after 24 h indicating no
186 protein interaction with the micellar surface.

187

CMC plots dPGS-SS-PCL/PLA/PLGA micelles in PBS at 37 °C by DLS

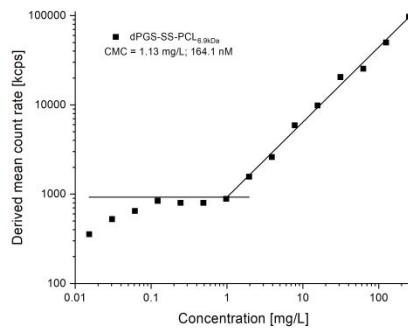


Figure S 29. CMC plot of dPGS_{3.0}-SS-PCL_{3.8}.

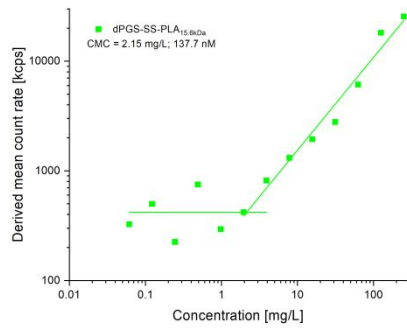


Figure S 30. CMC plot of dPGS_{7.8}-SS-PLA_{7.8}.

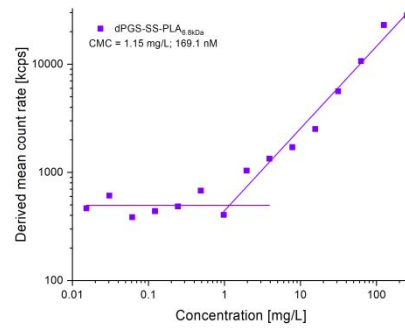


Figure S 31. CMC plot of dPGS_{3.0}-SS-PLA_{3.8}.

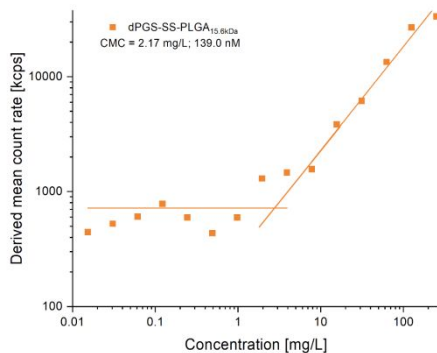


Figure S 32. CMC plot of dPGS_{7.8}-SS-PLGA_{7.8}.

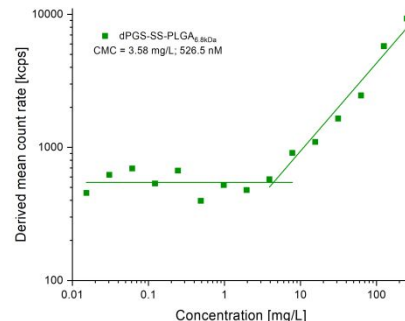
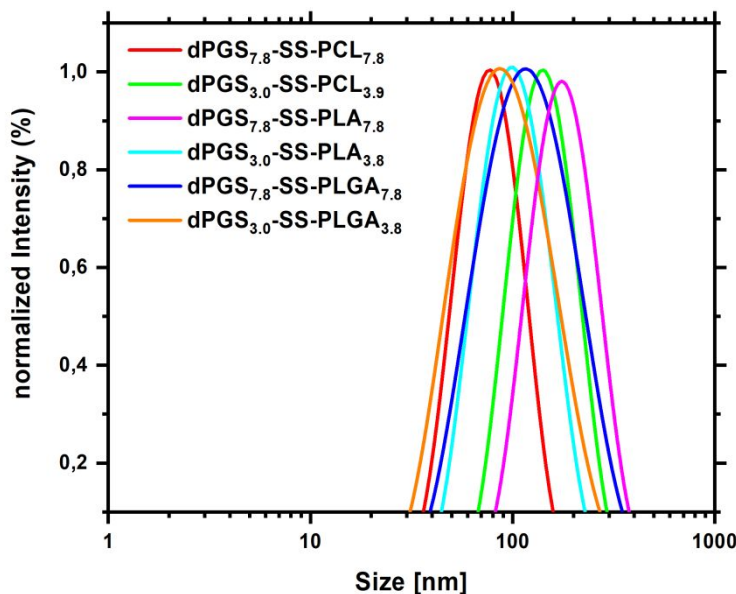


Figure S 33. CMC plot of dPGS_{3.0}-SS-PLGA_{3.8}.

189

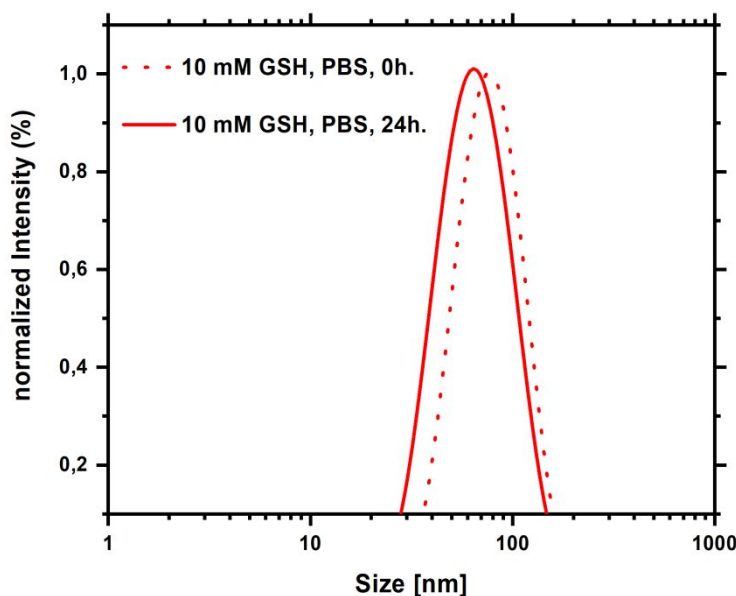
Size distributions of dPGS-SS-PCL/PLA/PLGA micelles: DLS plot



190

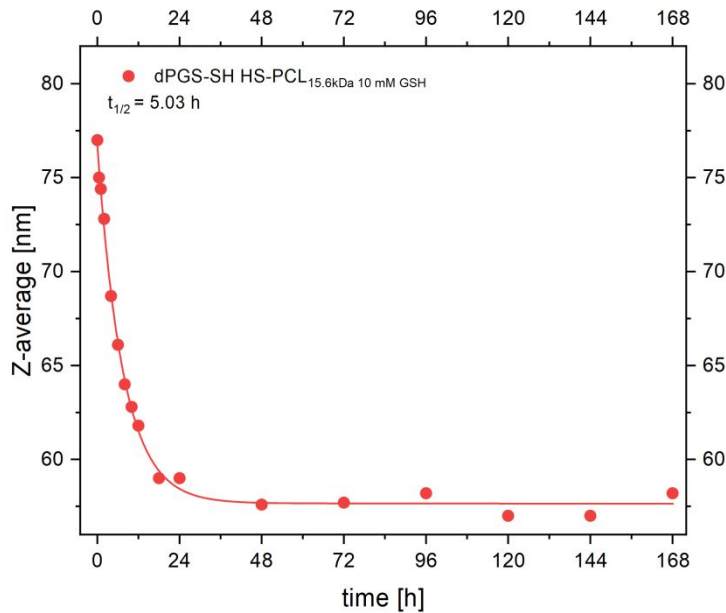
Figure S 34. the size distribution of dPGS-SS-PCL/PLA/PLGA micelles in PBS at 1 mg/mL.

Degradation in the presence of 10 mM GSH in PBS at 37 °C



194

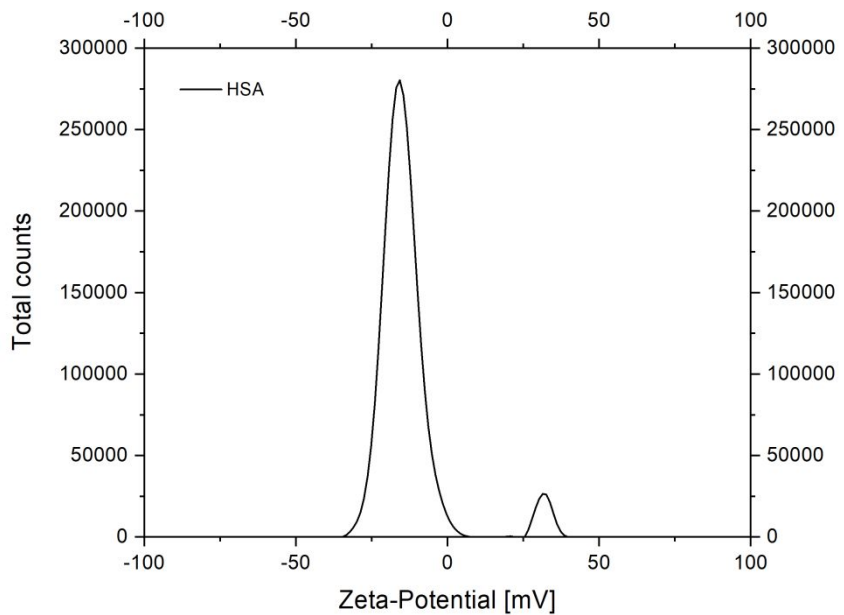
Figure S 35. the size distribution of dPGS_{7,8}-SS-PCL_{7,8} micelles in the presence of 10 mM GSH after 24 h at 37 °C.



197
198 **Figure S 36.** time-depended size evolution of dPGS_{7.8}-SS-PCL_{7.8} in the presence
199 of 10 mM GSH.

200
201
202 **Table S 6.** pH dependency of shell-shedding of micelles; neutral pH shows a higher
203 count rate indication higher particle concentration.

Compound	pH	Count rate (kcps)
10 mM GSH, PBS	7.4	33920
10 mM GSH, PBS	5.5	25140



205
206 **Figure S 37.** Zeta-potential of HSA ($c = 10 \text{ mg/mL}$) in PB buffer pH 7.4.
207

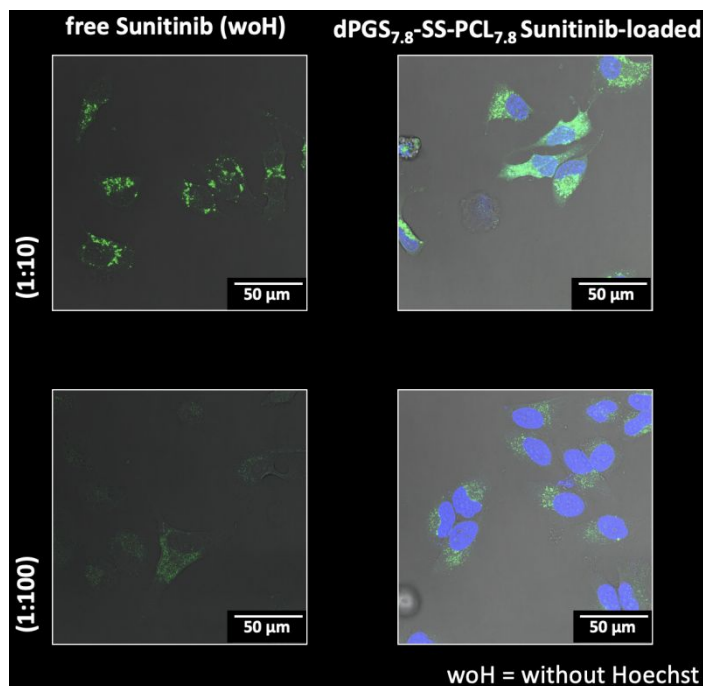
208 **Drug-Loading: Sunitinib-loaded micelles purified with SEC column (photography)**



209
210 **Figure S 38.** SEC of dPGS-SS.micelles to separate non-encapsulated drugs (Sunitinib) in
211 full view; Sunitinib-loaded micelles were loaded on the column and the yellow band was
212 collected.

213
214

Cellular Uptake of free Sunitinib and loaded in dPGS_{7.8}-SS-PCL_{7.8} micelles on HeLa cells

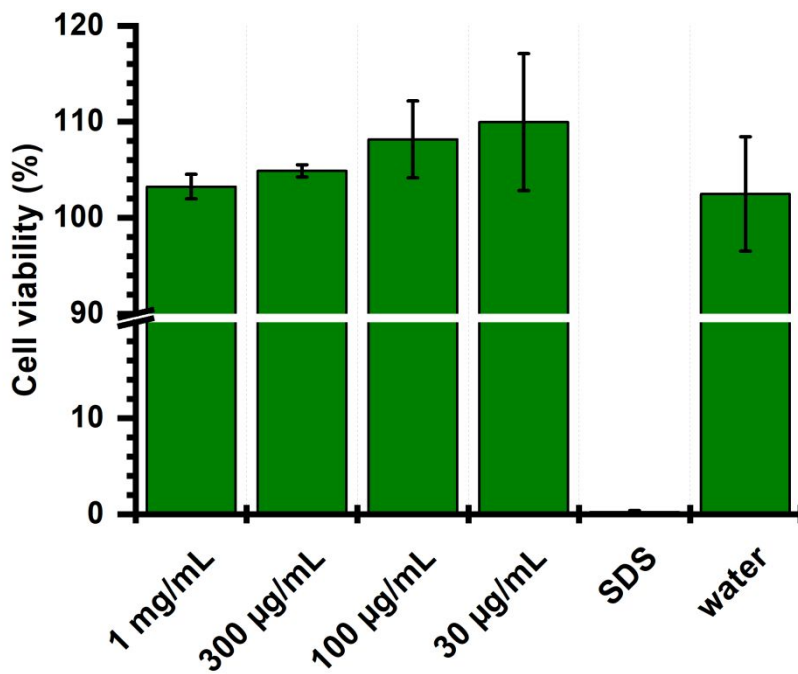


215
216
217

Figure S39. Cellular uptake on HeLa cells of free Sunitinib and Sunitinib-loaded dPGS_{7.8}-SS-PCL_{7.8} micelles with Hoechst staining after 24 h incubation.

218

Cell viability on A549 cell line dPGS_{7.8}-SS-PCL_{7.8}



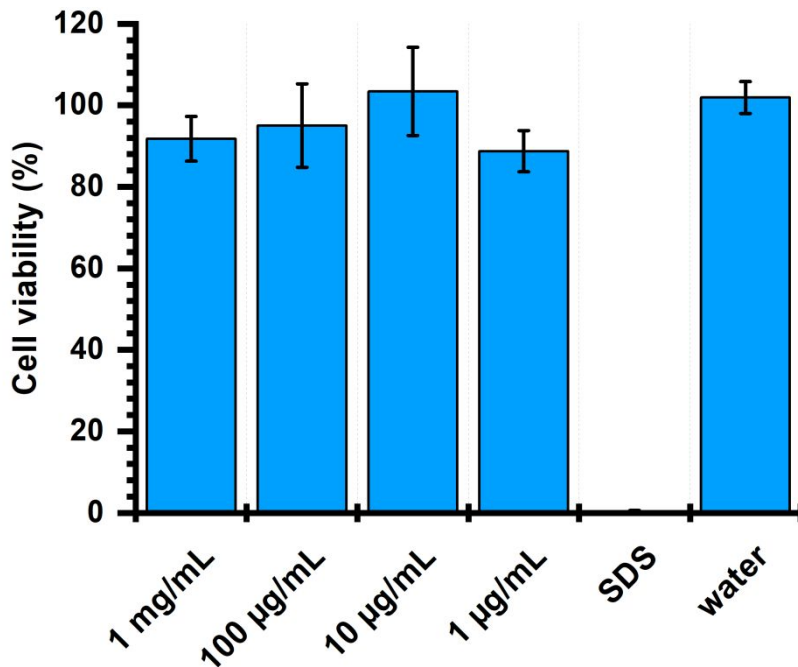
219

220
221

Figure S 40. CCK-8 assay on A549 cell lines for cell combability of empty dPGS_{7.8}-SS-PCL_{7.8} micelles (48 h, n=3).

222

Cell viability on Vero E6 cell line dPGS_{7.8}-SS-PCL_{7.8}



223

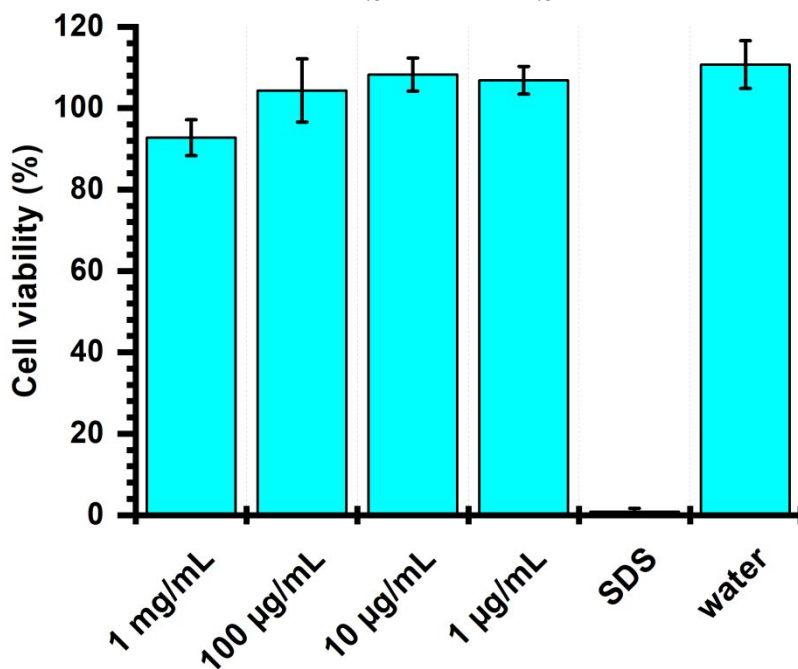
224

225

Figure S 41. CCK-8 assay on Vero E6 cell lines for cell combability of empty dPGS_{7.8}-SS-PCL_{7.8} micelles (24 h, n=3).

226

Cell viability on HBE cell line dPGS_{7.8}-SS-PCL_{7.8}



227

228

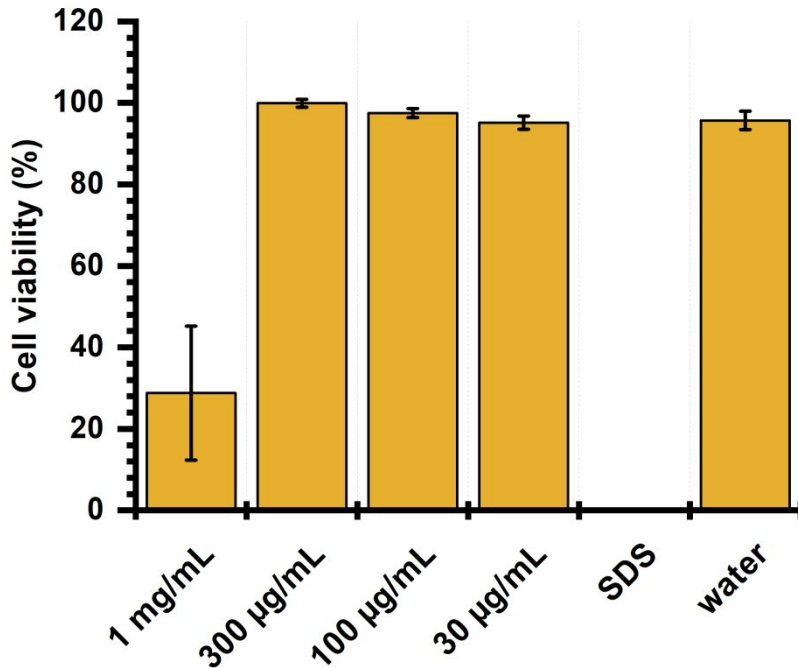
229

Figure S 42. CCK-8 assay on HBE cell lines for cell combability of empty dPGS_{7.8}-SS-PCL_{7.8} micelles (24 h, n=3).

230

231

Cell viability on L929 cell line dPGS_{7.8}-SS-PCL_{7.8}



232

233

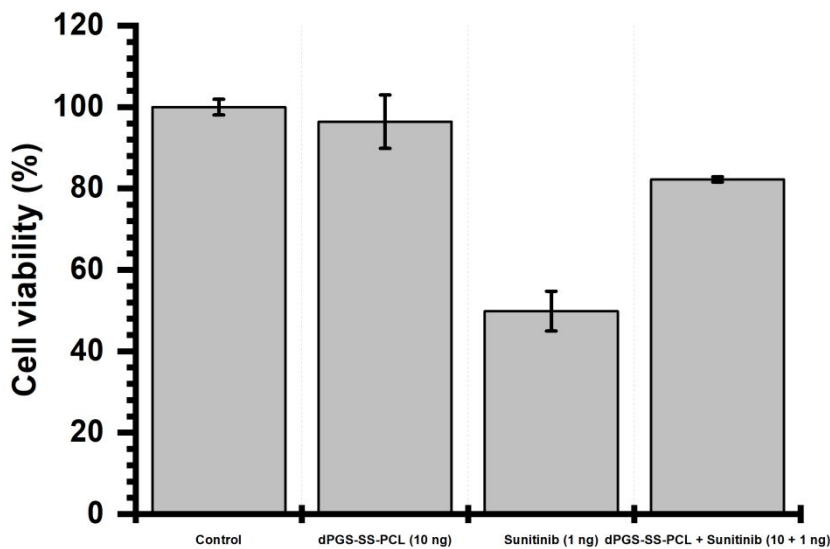
Figure S 43. CCK-8 assay on L929 cell lines for cell combability of empty dPGS_{7.8}-SS-PCL_{7.8} micelles (48 h, n=3).

234

235

Cell viability on HUVEC cell line dPGS_{7.8}-SS-PCL_{7.8} (Anti-Angiogenesis Assay)

236



237

238

Figure S 44. CCK-8 assay on HUVEC cell lines for cell combability of empty dPGS_{7.8}-SS-PCL_{7.8} micelles, free Sunitinib and Sunitinib-loaded micelles (4 h, triplicate).

239

241 References

- 243 1. Tanzi, M. C.; Verderio, P.; Lampugnani, M. G.; Resnati, M.; Dejana, E.; Sturani, E., Cytotoxicity
244 of some catalysts commonly used in the synthesis of copolymers for biomedical use. *J. Mater. Sci.: Mater. Med.* **1994**, 5 (6), 393-396.
245
- 246 2. Dzienia, A.; Maksym, P.; Hachuła, B.; Tarnacka, M.; Biela, T.; Golba, S.; Zięba, A.;
247 Chorążewski, M.; Kaminski, K.; Paluch, M., Studying the catalytic activity of DBU and TBD upon
248 water-initiated ROP of ε-caprolactone under different thermodynamic conditions. *Polym. Chem.*
249 **2019**, 10 (44), 6047-6061.
250
- 251 3. Kamber, N. E.; Jeong, W.; Waymouth, R. M.; Pratt, R. C.; Lohmeijer, B. G. G.; Hedrick, J. L.,
Organocatalytic Ring-Opening Polymerization. *Chem. Rev.* **2007**, 107 (12), 5813-5840.
252
- 253 4. Dove, A. P., Organic Catalysis for Ring-Opening Polymerization. *ACS Macro Lett.* **2012**, 1 (12),
1409-1412.
254
- 255 5. Lohmeijer, B. G. G.; Pratt, R. C.; Leibfarth, F.; Logan, J. W.; Long, D. A.; Dove, A. P.;
Nederberg, F.; Choi, J.; Wade, C.; Waymouth, R. M.; Hedrick, J. L., Guanidine and Amidine
256 Organocatalysts for Ring-Opening Polymerization of Cyclic Esters. *Macromolecules* **2006**, 39 (25),
8574-8583.
257
- 258 6. Qian, H.; Wohl, A. R.; Crow, J. T.; Macosko, C. W.; Hoye, T. R., A Strategy for Control of
“Random” Copolymerization of Lactide and Glycolide: Application to Synthesis of PEG-b-PLGA
259 Block Polymers Having Narrow Dispersity. *Macromolecules* **2011**, 44 (18), 7132-7140.
260
- 261 7. Wilms, D.; Stiriba, S.-E.; Frey, H., Hyperbranched Polyglycerols: From the Controlled Synthesis of
Biocompatible Polyether Polyols to Multipurpose Applications. *Acc. Chem. Res.* **2010**, 43 (1), 129-
141.
262
- 263 8. Sunder, A.; Hanselmann, R.; Frey, H.; Mülhaupt, R., Controlled Synthesis of Hyperbranched
Polyglycerols by Ring-Opening Multibranching Polymerization. *Macromolecules* **1999**, 32 (13),
4240-4246.
264
- 265
- 266